nature microbiology

LETTERS

PUBLISHED: 12 DECEMBER 2016 | VOLUME: 2 | ARTICLE NUMBER: 16237

CozE is a member of the MreCD complex that directs cell elongation in *Streptococcus pneumoniae*

Andrew K. Fenton, Lamya El Mortaji, Derek T. C. Lau, David Z. Rudner* and Thomas G. Bernhardt*

Most bacterial cells are surrounded by a peptidoglycan cell wall that is essential for their integrity. The major synthases of this exoskeleton are called penicillin-binding proteins (PBPs)[1,2]. Surprisingly little is known about how cells control these enzymes, given their importance as drug targets. In the model Gram-negative bacterium *Escherichia coli*, outer membrane lipoproteins are critical activators of the class A PBPs (aPBPs)[3,4], bifunctional synthases capable of polymerizing and crosslinking peptidoglycan to build the exoskeletal matrix[1]. Regulators of PBP activity in Gram-positive bacteria have yet to be discovered but are likely to be distinct due to the absence of an outer membrane. To uncover Gram-positive PBP regulatory factors, we used transposon-sequencing (Tn-Seq)[5] to screen for mutations affecting the growth of *Streptococcus pneumoniae* cells when the aPBP synthase PBP1a was inactivated. Our analysis revealed a set of genes that were essential for growth in wild-type cells yet dispensable when *pbp1a* was deleted. The proteins encoded by these genes include the conserved cell wall elongation factors MreC and MreD[2,6,7], as well as a membrane protein of unknown function (SPD_0768) that we have named CozE (coordinator of zonal elongation). Our results indicate that CozE is a member of the MreCD complex of *S. pneumoniae* that directs the activity of PBP1a to the midcell plane where it promotes zonal cell elongation and normal morphology. CozE homologues are broadly distributed among bacteria, suggesting that they represent a widespread family of morphogenic proteins controlling cell wall biogenesis by the PBPs.

To investigate PBP regulation in Gram-positive organisms we used the ellipsoid-shaped bacterium *S. pneumoniae* as a model system. In addition to its interesting morphology, this bacterium is an important human pathogen and the causative agent of many invasive diseases. Antibiotic resistance in *S. pneumoniae* is on the rise worldwide[8]. New drugs to combat resistance in this and other bacterial pathogens are therefore needed. A better understanding of the regulation and cellular function of proven target enzymes like the penicillin-binding proteins (PBPs) will aid the development of such therapies.

S. pneumoniae encodes three aPBPs (*pbp1a*, *pbp1b* and *pbp2a*), with *pbp1a* and *pbp2a* forming an essential pair. Either gene can be deleted individually, but attempts to inactivate both genes have been unsuccessful[9]. We reasoned that the lethal phenotype of *pbp1a pbp2a* double mutants could form the basis of a screen for Gram-positive PBP regulators analogous to previous work that identified the Lpo regulators of the *E. coli* Class A PBPs (aPBPs)[4]. The set of mutants synthetically lethal with a deletion of *pbp1a* is predicted to include factors required for the *in vivo* function of PBP2a. Similarly, a screen for mutants synthetically lethal with Δ*pbp2a* should identify factors required for PBP1a activity. To identify synthetic interactions, we performed Tn-Seq (IN-Seq, HITS, TraDIS)[5,10,11] using transposon libraries generated in strain D39 lacking its capsule (Δ*cps*)[7] and derivatives inactivated for PBP1a and PBP2a. This approach revealed several factors, which will be investigated in a separate report. Here, we focus on the characterization of an unexpected class of factors with a distinct and intriguing phenotype related to PBP1a, an aPBP that is associated with high-level antibiotic resistance[12] and is indispensable for host colonization[13]. The genes encoding these proteins were found to be virtually devoid of insertions in the wild-type transposon library, indicating they are probably essential for growth (Fig. 1a and Supplementary Fig. 1). Strikingly, however, the same genes appeared to be readily inactivated in the Δ*pbp1a* library but not the Δ*pbp2a* library (Fig. 1a and Supplementary Fig. 1), suggesting that *pbp1a* disruption suppresses their essentiality. Two of the genes encode MreC and MreD, conserved members of the peptidoglycan (PG) biogenesis machinery that promotes cell elongation in rod- and ellipsoid-shaped bacteria[2,6,7]. The third gene, *spd_0768*, encodes CozE, a conserved polytopic membrane protein of unknown function that belongs to the widely distributed UPF0118 protein family[14] (Fig. 1a–c and Supplementary Figs 2 and 3). Like MreC, CozE homologues are absent from the Mollicutes, which lack a cell wall, suggesting a role for CozE in PG biosynthesis (Supplementary Fig. 3).

The essentiality of *mreC* and *mreD* and its suppression by PBP1a inactivation were expected from earlier work by Winkler and colleagues[7,15]. We confirmed these results using a Δ*pbp1a* strain with an ectopic copy of *pbp1a* under control of a zinc-regulated promoter[16] (P_{zn}::*pbp1a*). In this strain background, deletion mutants of *mreC*, *mreD* and *cozE*, or both *mreC* and *cozE*, were viable in the absence of zinc (Fig. 1d and Supplementary Fig. 4). However, the viability of these strains was severely compromised on solid medium supplemented with zinc (Fig. 1d and Supplementary Fig. 4). As an additional confirmation, we deleted *mreC* or *cozE* in strain R6, which harbours a hypomorphic *pbp1a* allele[17], and found that both mutants were viable, displaying only mild morphological defects (Supplementary Fig. 5a)[7]. Furthermore, expression of the *pbp1a* gene from strain D39 was lethal in *mreC* or *cozE* R6 deletion mutants (Supplementary Fig. 5b). In liquid culture, *pbp1a* induction was tolerated in wild-type (wt) or Δ*pbp1a* cells of strain D39, but caused cell lysis in Δ*pbp1a* Δ*mreC* and Δ*pbp1a* Δ*cozE* double mutants as well as the Δ*pbp1a* Δ*mreC* Δ*cozE* triple mutant (Fig. 2a,b and Supplementary Fig. 6b). Upon *pbp1a* induction, these mutants first displayed a cell chaining phenotype followed by significant rounding and swelling of cells in the chains before most cells in the culture lysed (Fig. 2b and Supplementary Fig. 6d). Similar phenotypes were observed upon CozE or MreCD depletion in an otherwise wild-type background (Supplementary Fig. 7)[7]. The PBP1a-induced lysis phenotype appeared to be more pronounced in cells lacking both CozE and MreC (Fig. 2a). However, the drop in viability for single *mreC* or *cozE* mutants was similar to that of the double mutant (Supplementary Fig. 6c),

Department of Microbiology and Immunobiology, Harvard Medical School, Boston, Massachusetts 02115, USA. *e-mail: david_rudner@hms.harvard.edu; thomas_bernhardt@hms.harvard.edu

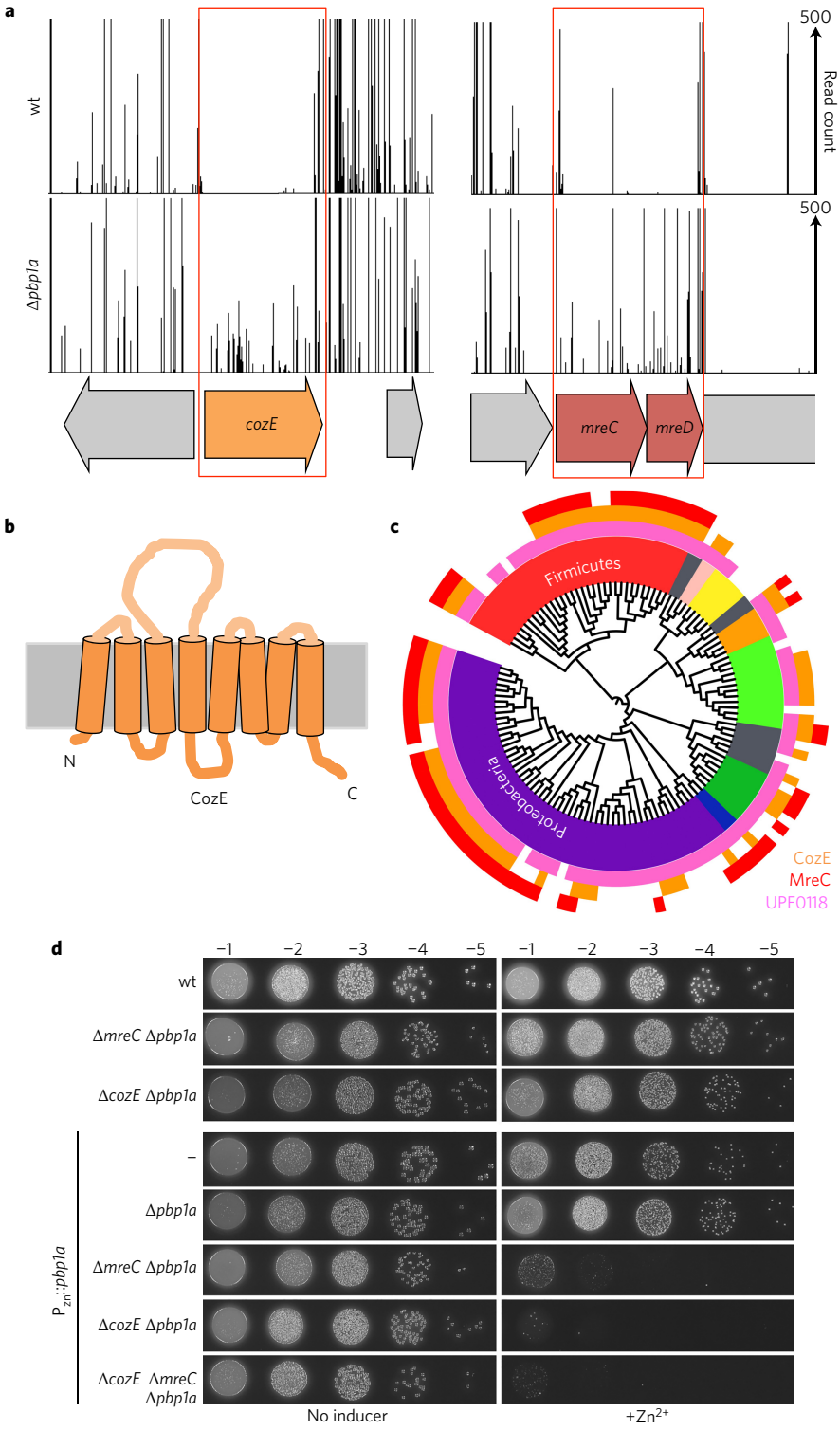

Figure 1 | The essential genes *cozE* and *mreCD* can be deleted in cells lacking PBP1a. a, Mariner transposon libraries were generated in wt (D39 Δ*cps*) and Δ*pbp1a* mutant strains. Transposon insertions in each library were identified by deep sequencing and mapped onto the D39 genome. The height of each line reflects the number of sequencing reads at this position. Boxes highlight loci significantly enriched ($P < 0.002$) for transposon insertions in the Δ*pbp1a* library compared to wt. Full Tn-Seq and statistical data are provided in Supplementary Fig. 1. **b**, Schematic of the predicted membrane topology of CozE adapted from topological predictions using the Phobius web server. Raw data output is provided in Supplementary Fig. 2a. **c**, CozE proteins are widely conserved and co-occur with MreC. The tree shows 129 diverse bacterial species. UPF0118 family proteins (pink), CozE (orange) and MreC (red) family members are indicated (*e*-value cutoff = 1×10^{-4}). A tree with all phyla and leaves labelled is provided in Supplementary Fig. 2b. A larger tree with 1,576 bacterial species is provided in Supplementary Fig. 3. **d**, The essentiality of *cozE* and *mreC* can be suppressed by depletion of PBP1a. A spot dilution series of indicated strains in the presence and absence of an inducer is shown. Strains were grown to exponential phase, normalized to an OD_{600} of 0.2, serially diluted and 5 µl of each was spotted onto TSAII 5%SB plates in the presence or absence of 600 µM $ZnCl_2$. Representative images of two replicates are shown. Spot dilutions showing Δ*mreD* and Δ*mreCD* essentiality and its suppression by depletion of PBP1a are presented in Supplementary Fig. 4.

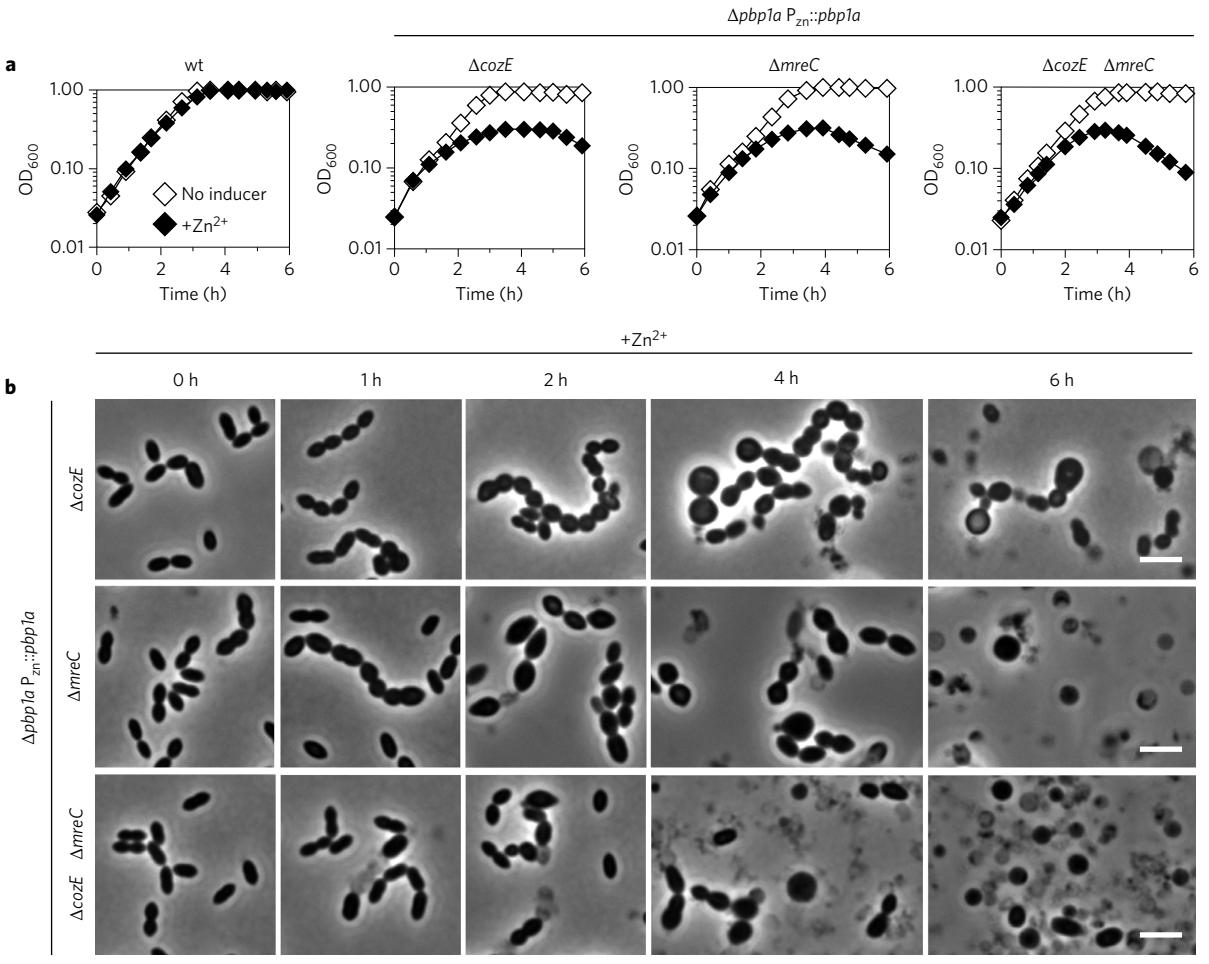

Figure 2 | Expression of PBP1a in cells lacking *cozE* or *mreC* leads to growth arrest, aberrant morphologies and lysis. a, Growth curves of indicated strains in the presence and absence of an inducer. Strains were grown in THY to mid-exponential phase at 37 °C in 5% CO_2 and back-diluted in fresh THY to an OD_{600} of 0.025 in the presence or absence of 600 μM $ZnCl_2$, with the optical density monitored over time. Growth curves are representative of at least three replicates. Growth curves of additional deletion strains and P_{zn}::*pbp1a* overexpression controls are provided in Supplementary Fig. 6b. Viable counts of cultures at 6 and 8 h post-induction are reported in Supplementary Fig. 6c. **b**, Representative images of Δ*cozE*, Δ*mreC* and Δ*cozE* Δ*mreC* strains upon induction of P_{zn}::*pbp1a*. Strains were grown as in **a**. At the indicated times after the addition of the inducer, cells were imaged by phase-contrast microscopy on THY 2% agarose pads. Images of strains in the absence of the inducer are shown in Supplementary Fig. 6d. Images of deletion strains lacking the P_{zn}::*pbp1a* construct are shown in Supplementary Fig. 6a. All images are representative of at least four replicates. Scale bars, 3 μm.

suggesting that these factors function in the same pathway. Deletion of *lytA* or *cbpD* encoding the major *S. pneumoniae* autolysins did not dramatically alter the lytic effect of PBP1a production in the absence of CozE or MreC, indicating that the growth and lysis phenotypes did not result from misactivation of these autolysins[18,19] (Supplementary Fig. 8).

The genetic results suggest a model in which CozE works with the MreCD complex to control PG synthesis by PBP1a and that, in their absence, deranged PBP1a activity causes cell lysis. To test this possibility, we monitored PG biogenesis activity using the fluorescent D-amino acid TADA (tetramethylrhodamine 3-amino-D-alanine)[20,21] and the localization of a functional GFP-PBP1a fusion (Supplementary Fig. 9) in cells inactivated for CozE or MreC. As with the untagged version, production of GFP-PBP1a in cells lacking MreC or CozE resulted in a severe growth defect (Fig. 3a and Supplementary Fig. 10a). This phenotype was accompanied by a change in GFP-PBP1a localization and TADA labelling from their normally tightly restricted zone at midcell to a widely distributed pattern throughout the cell periphery. The Δ*mreC* cells displayed a more severe labelling defect versus Δ*cozE* cells, as expected from the above morphological analysis (Fig. 3b,c and Supplementary Fig. 11). Similar alterations in TADA labelling were observed following the production of untagged PBP1a in the mutant strains (Supplementary Fig. 12). Importantly, variants of GFP-PBP1a inactivated for either PG polymerase/glycosyltransferase activity [GFP-PBP1a(GT^-)] or PG crosslinking/transpeptidase activity [GFP-PBP1a(TP^-)] similarly lost their midcell localization in cells lacking CozE or MreC, but this delocalization was not associated with a change in TADA labelling nor did it cause a significant growth defect (Fig. 3b,c and Supplementary Fig. 10a). Cells lacking CozE or MreC did not affect midcell localization of GFP-PBP2a, suggesting a specific role in PBP1a recruitment (Supplementary Fig. 13).

A functional GFP-CozE fusion (Supplementary Fig. 7a) displayed a septal localization pattern that was dependent on MreC (Fig. 4a and Supplementary Fig. 14). Reciprocally, the midcell localization of GFP-MreC required CozE (Supplementary Fig. 14). Moreover, bacterial two-hybrid analysis[22] in *E. coli* indicates that CozE forms a complex with MreCD and PBP1a (Fig. 4b and Supplementary Fig. 15). Finally, a functional FLAG-CozE fusion was co-immunoprecipitated with GFP-PBP1a but not GFP-PBP2a (Fig. 4c and Supplementary Fig. 16). Altogether, these data indicate that CozE is a member of the MreCD morphogenic complex in *S. pneumoniae* and that this complex coordinates

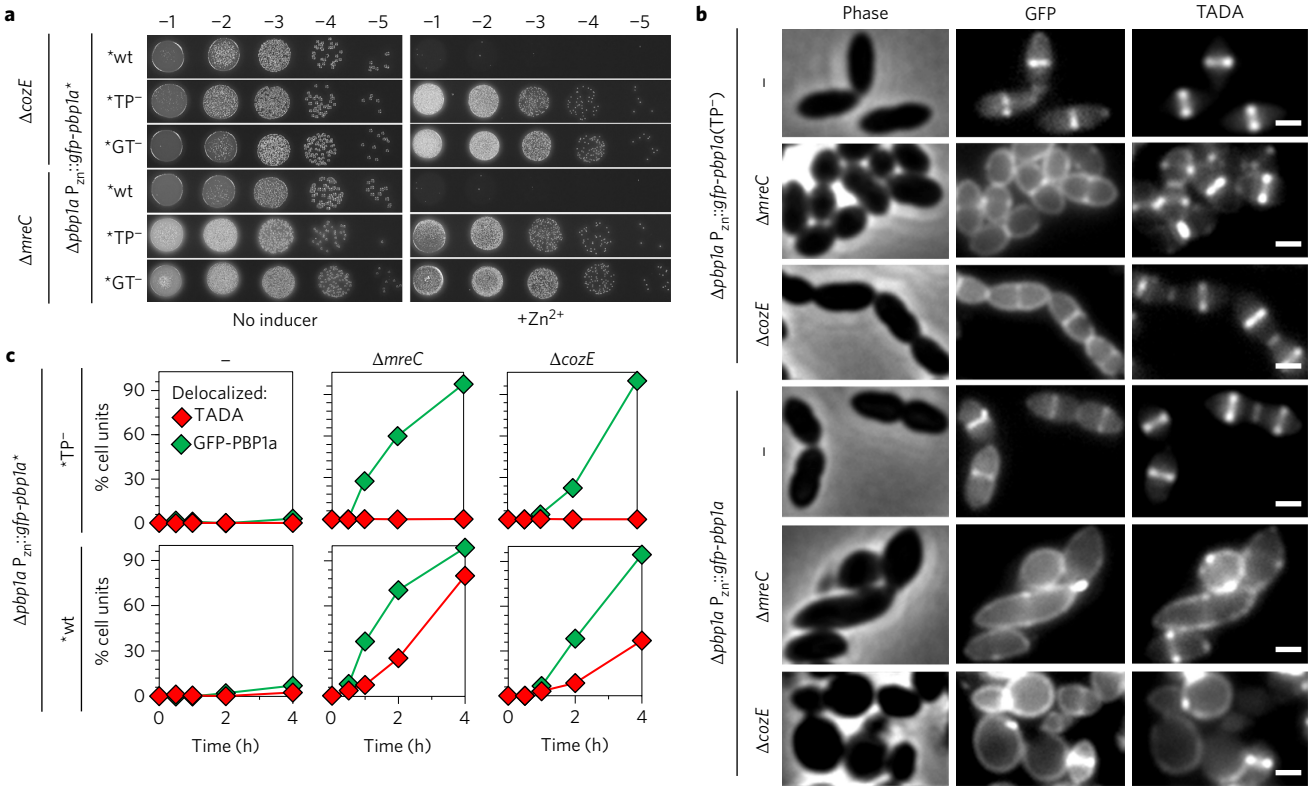

Figure 3 | PBP1a-dependent PG synthesis is delocalized in the absence of CozE or MreC. a, Cells lacking CozE or MreC are viable if PBP1a lacks its enzymatic activities. A spot dilution series of indicated strains in the presence and absence of 600 μM $ZnCl_2$ is shown. The Δ*cozE* and Δ*mreC* mutants fail to grow when GFP-PBP1a is induced but retain viability when glycosyltransferase (GT^-) or transpeptidase (TP^-)-defective variants are expressed. Representative images of two replicates are shown. **b**, Aberrant GFP-PBP1a localization and TADA labelling in Δ*cozE* and Δ*mreC* strains. Representative images of indicated strains grown to mid-exponential phase, back-diluted to an OD_{600} of 0.025 in THY + 600 μM $ZnCl_2$ and incubated at 37 °C in 5% CO_2 for 3 h 45 min. When necessary, cultures were back-diluted at 2 h to avoid high cell densities and autolysis. Cell wall synthesis was monitored by the addition of TADA for 15 min before imaging. Representative images of at least two replicates are shown. Scale bars, 1 μm. Assays for GFP-PBP1a functionality are provided in Supplementary Fig. 9. Growth curves showing that GFP-PBP1a expression in Δ*cozE* and Δ*mreC* strains leads to lysis are presented in Supplementary Fig. 10a. Immunoblot analyses of GFP-PBP1a expression levels are provided in Supplementary Fig. 10b. GFP-PBP1a (GT^-) has a similar phenotype to the GFP-PBP1a (TP^-) mutant shown here (Supplementary Fig. 10c). **c**, Quantification of GFP-PBP1a localization and TADA incorporation patterns in Δ*cozE* and Δ*mreC* strains. Strains containing P_{zn}::*gfp-pbp1a* or a catalytically inactive variant (TP^-) were treated as described in **b**. Cells were imaged and scored for localization/incorporation at the indicated time. Each cell in the joined diplococcus was treated as a single cell unit and scored as wt mid-cell localized signal or delocalized signal. The percentages of cells with delocalized signal for TADA or GFP-PBP1a localization in the indicated strains are shown. More than 700 cell units were scored per time point ($n = 2$). Demograms of GFP-PBP1a and TADA signal profiles at the 4 h time point are provided in Supplementary Fig. 11. Similar TADA labelling to that shown in **b** and **c**, using untagged PBP1a, is provided in Supplementary Fig. 12.

cell elongation in part by interacting with and restricting PBP1a to the midcell (Fig. 4d).

In rod-shaped bacteria, MreC and MreD are part of the Rod system, which elongates the cylindrical portion of the cell wall[23]. The system is organized by dynamic filaments of MreB that facilitate the incorporation of PG at dispersed locations throughout the cylinder[24]. In contrast, *S. pneumoniae* and other ovococci elongate in a restricted zone by incorporating PG at the periphery of the cytokinetic ring[25]. These bacteria lack MreB, but retain the other components of the Rod system, including MreC and MreD. It was recently shown that the shape, elongation, division and sporulation (SEDS)-family protein RodA is the core PG polymerase within the Rod system of *Bacillus subtilis* and *E. coli*[26,27]. Additionally, it was found that although aPBP polymerases principally work outside the MreB-directed machinery, the two systems display some interdependence through an as yet ill-defined coordination mechanism[27]. The results presented in this report suggest the possibility that CozE and related proteins might serve as part of this coordination mechanism by connecting PBP1a with RodA and other components of the elongation machinery via its interactions with PBP1a and the MreCD complex. In this case, CozE may be essential in *S. pneumoniae* because the spatial localization of aPBPs and their potential coordination with SEDS-family PG polymerases is especially critical for proper PG biogenesis in organisms where zonal cell wall expansion is the principal mode of growth. Such a localized mode of cell elongation is not unique to the ovococci. In addition to the dispersed mode of growth promoted by the Rod system, rod-shaped bacteria like *E. coli* and *Caulobacter crescentus* have also been found to undergo zonal elongation for a portion of the cell cycle preceding division[28–30]. The broad conservation of CozE suggests that it could more generally recruit and coordinate PG synthetic functions during zonal growth in a range of bacteria. Further characterization of CozE in S. pneumoniae and other organisms will provide deeper mechanistic insight into its function and reveal new strategies for disrupting PG biogenesis for antibiotic development.

Methods

Strains, plasmids and routine growth conditions. Unless otherwise indicated, all *S. pneumoniae* strains in this study were derived from D39 Δ*cps* (ref. 17) or R6 (refs 17,31,32), a non-pathogenic derivative of D39. Cells were grown in Todd Hewitt broth containing 0.5% yeast extract (THY) at 37 °C in an atmosphere containing 5% CO_2. Strains were grown on pre-poured tryptic soy agar 5% sheep blood plates (TSAII 5%SB, Becton Dickinson) with a 5 ml overlay of 1% nutrient

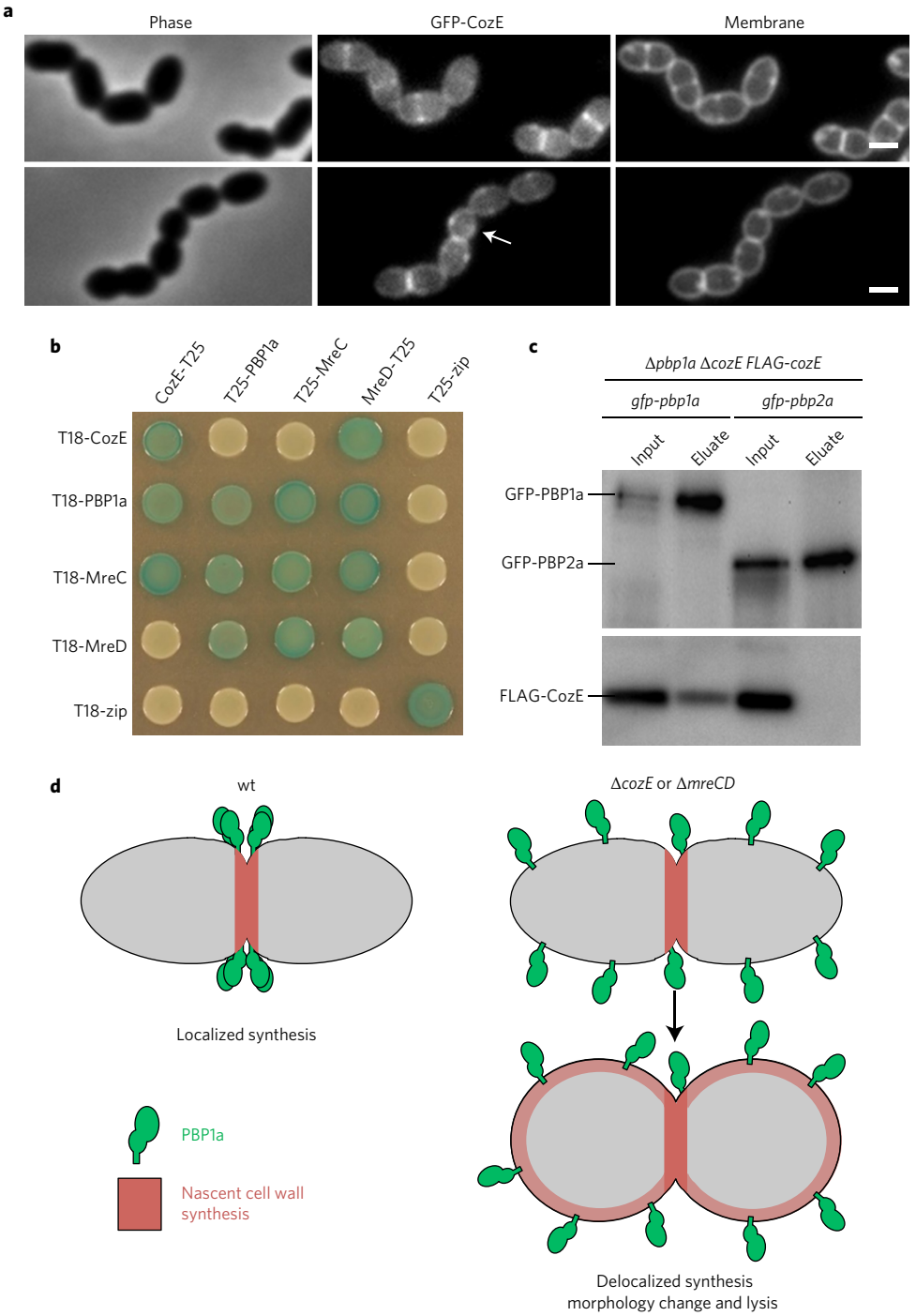

Figure 4 | CozE is a member of the MreCD cell elongation complex. a, CozE is enriched at mid-cell. *S. pneumoniae* cells expressing GFP-CozE under the control of a fucose-inducible promoter were grown to mid-exponential phase in THY + 0.4% fucose, spotted onto 2% agarose pads and imaged. In rare cases, GFP-CozE can be detected at mid-cell before the onset of membrane invagination (white arrow). Two representative images are shown ($n = 3$). Scale bars, 1 μm. **b**, Bacterial two-hybrid interactions of CozE with members of the PG biosynthetic complex. *E. coli* strain BTH101 (Δ*cya*) expresses protein fusions to domains (T25 and T18) of adenylate cyclase. Positive interactions reunite T25 and T18 domains, resulting in *lacZ* expresses and blue colonies on LB agar containing X-gal. Strains were grown to stationary phase in LB at 30 °C and 5 μl volumes were spotted onto LB agar plates supplemented with X-gal, incubated at 30 °C and imaged. The 'zip' fusions are to a leucine zipper domain derived from the yeast protein GCN4 and serve as both positive and negative controls. A representative image from three biological replicates is shown. Additional controls are provided in Supplementary Fig. 15. **c**, A functional FLAG-CozE fusion co-immunoprecipitates with GFP-PBP1a but not GFP-PBP2a. Digitonin-solubilized membrane preparations from the indicated strains were incubated with anti-GFP resin, washed and eluted in a sample buffer. Immunoblots show matched samples of solubilized membrane (input) and elution (eluate, 20 × concentrated relative to input), fractions were probed with anti-GFP and anti-FLAG antibodies. Representative blots are shown ($n = 4$). Evidence of FLAG-functionality, antibody specificity and full immunoblot analysis is provided in Supplementary Fig. 16. An untagged PBP1a control showing that FLAG-CozE does not precipitate with the resin is presented in Supplementary Fig. 16c. **d**, Schematic model of CozE and MreCD function. In wt cells, the PBP1a (green) is held at mid-cell by the CozE/MreCD complex, resulting in nascent cell wall synthesis at this location (red shading). In the absence of CozE or MreCD, PBP1a catalyses delocalized PG synthesis, causing lethal morphological defects.

broth (NB) agar containing additives. When finer control of media components was required, TSA plates containing 5% defibrinated sheep blood were used. All strains, plasmids and oligonucleotides used in this study are provided in Supplementary Tables 1–4.

Transformation. Cells in mid-exponential phase were grown in THY and back-diluted to an optical density at 600 nm (OD_{600}) of 0.03. Competence was induced with 500 pg ml^{-1} competence stimulating peptide (CSP-1), 0.2% BSA and 1 mM $CaCl_2$. Typically, 1 ml of culture was transformed with 100 ng of gDNA or plasmid DNA. Transformants were selected on TSAII overlay plates containing 5 μg ml^{-1} chloramphenicol, 0.2 μg ml^{-1} erythromycin, 250 μg ml^{-1} kanamycin, 200 μg ml^{-1} spectinomycin or 0.2 μg ml^{-1} tetracycline, as appropriate.

S. pneumoniae strain construction

S. pneumoniae deletion strains. All *S. pneumoniae* deletion strains were generated using linear PCR fragments, similar to the method used by Robertson and co-authors[33]. Two ~1 kb flanking regions of each target gene were PCR amplified and an antibiotic resistance marker placed between them using isothermal assembly[34]. Assembled PCR products were transformed directly into *S. pneumoniae* as described above. In all cases, deletion primers were given the typical name 'gene-designation'_5FLANK_F/R for 5′ regions and 'gene-designation'_3FLANK_F/R for 3′ regions. Antibiotic markers were amplified from Δ*bgaA* strains using the AntibioticMarker_F/R primers using gDNA isolated from strains: AKF_Spn001-005. A full list of primer sequences is provided in Supplementary Table 4. Transformants were picked into 5 ml THY, grown to exponential phase and frozen without undergoing autolysis. Deletion strains were confirmed by diagnostic PCR using the AntibioticMarker_R primer in conjunction with a primer binding ~100 bp 5′ of the disrupted gene. These primers were given the typical name 'ORFdesigation'_Seq_F. Diagnostic PCRs gave ~2–2.5 kb PCR products, depending on the marker, which was not present in wt controls.

Confirmed gDNA preparations of single gene deletions were diluted to 20 ng μl^{-1} and used for the construction of multiple knockout strains. For strains containing multiple deletions and construct integrations, transformants were verified by diagnostic re-streaking on media containing antibiotics. In special cases where more confidence was desirable, each construct was confirmed by diagnostic PCR.

Antibiotic-marked ΔbgaA strains. Strains containing a variety of antibiotic resistance cassettes inserted at the *bgaA* locus served as the source of all markers used in this study. In all cases, cassettes were modified to make them compatible with amplification by the AntibioticMarker_F and AntibioticMarker_R primers. This has the advantage of all antibiotic markers being compatible with a single set of primers, which makes cloning and antibiotic marker replacement a simple process.

For construction of the *bgaA* PCR knockout constructs, the chloramphenicol resistance cassette was amplified from pAC1000 (ref. 35) using primers Chlor_isoT_F/R. The kanamycin and erythromycin resistance cassettes were amplified from pDR240 and pDR242, respectively, using primers AntibioticMarker_F/R. The *Janus* cassette was used as the original source of the kanamycin marker[36]. The spectinomycin resistance cassette was amplified from pMagellan6 (ref. 5) using primers Spec_isoT_F/R. Finally, the tetracycline resistance cassette was amplified from pJWV025 (ref. 37) using primers Tet_isoT_F/R. A 5′ flanking region of *bgaA* and a 3′ *bgaA* open reading frame (ORF) fragment was amplified using primers BgaA_5FLANK_F/R and BgaA_3ORF_F/R. Amplified *bgaA* fragments were combined with each resistance marker using isothermal assembly[34], transformed into *S. pneumoniae* and selected on media containing the appropriate antibiotic. Integration of each resistance cassette at the *bgaA* locus was confirmed by diagnostic PCR using the *bgaA* flanking primers *bgaA*_FLANK_F and AntibioticMarker_R. Resulting strains were given the names AKF_Spn001-005 (Supplementary Table 1).

P_{zn}::pbp1a. The P_{czc} promoter[16], henceforth known as P_{zn}, was amplified from pJW025 (ref. 37) using primers oSP104 and oSp105. The *pbp1a* ORF was amplified from the D39 genome using oSp106 and oSp107 and added to the first 'P_{zn}' fragment by isothermal assembly. The resulting product was digested with BamHI and XhoI and ligated into pLEM019 cut with the same enzymes. This resulted in the plasmid pAKF201, which contains the *pbp1a* ORF under the control of a zinc-inducible promoter with a consensus RBS. This construct was integrated into the D39 genome at the *bgaA* site using flanking regions of homology present in the pLEM019 vector. The P_{zn}::*pbp1a* construct was fully sequenced, linearized and transformed into *S. pneumoniae* for *bgaA* integration.

For *pbp1a* R6 expression (P_{zn}::$pbp1a^{R6}$) the P_{zn} promoter was amplified from pJW025[37] with oSP104 and oSp105 and the *pbp1a* ORF was amplified from the R6 genome using oSp106 and oSp107. The resulting PCR products were combined by isothermal assembly, digested with BamHI and XhoI and ligated into pLEM019 cut with the same enzymes. The resulting construct (pLEM025) was fully sequenced and the two expected variants (A370G and T1164G) confirmed.

P_{zn}::gfp-pbp1a. The whole pAKF201 plasmid was amplified using primers: PBP1a_GFP/YFP_N_3F2 and PBP1a_GFP/YFP_N_5R. This introduced overlapping regions for isothermal assembly and a short linker sequence (coding: LEGPAGL). The *gfp* ORF was amplified using primers GFP/YFP _N_F and GFP/YFP_N_R from pUC57-*gfp*. The pUC57-*gfp* plasmid contains a *de novo* synthesized *gfp* ORF, the sequence of which was originally from a *mut2 gfp* variant in pKL134 (ref. 38) but contains additional mutations, S65A, V68L, S72A and A206K (for momomerization). It has also been codon optimized for expression of *S. pneumoniae*. These two fragments were combined by isothermal assembly, resulting in pAKF214. This plasmid was sequenced and transformed into *S. pneumoniae*. Specific integration into the *bgaA* locus was confirmed by diagnostic PCR using the BgaA_FLANK_F primer.

Glycosyltransferase (GT^-) and transpeptidase (TP^-) defective pbp1a strains. Catalytic glycosyltransferase residues (E91A and E150A) were identified by alignment to the putative active site residues of *E. coli* PBP1b, identified by Sung and co-authors[39]. The catalytic serine in the PBP1a transpeptidase domain was identified through the conserved motifs and information from the PBP1a crystal structure[12]. In all cases, residues were mutagenized to a GCT alanine codon. P_{zn}::*pbp1a*(GT^-) was generated by two rounds of quick-change PCR, with primers pbp1a_E91A _F/R and pbp1a_E150 _F/R, resulting in pAKF213. P_{zn}::*pbp1a*(TP^-) was cloned with one round of quick-change PCR with primers pbp1a_S370A _F/R, resulting in pAKF212. P_{zn}::*gfp-pbp1a*(GT^-) was cloned by digesting pAKF213 with SpeI and XhoI, generating a *pbp1a* fragment containing the GT^- point mutations. This fragment was inserted into pAKF214 cut with the same enzymes, resulting in pAKF223. P_{zn}::*gfp-pbp1a*(TP^-) was cloned by mutagenic PCR using primers pbp1a_S370A _F/R, resulting in pAKF222. In all cases, point mutations were confirmed by sequencing. Plasmids were transformed into *S. pneumoniae* and specific integration into the *bga* locus was confirmed by diagnostic PCR using the BgaA_FLANK_F primer.

P_{zn}::pbp2a. The P_{zn} (ref. 16) promoter was amplified from pJW025 (ref. 37) using primers oSP104 and oSp105. The *pbp2a* ORF was amplified from the D39 genome using oSp108 and oSp109 and added to the first fragment by isothermal assembly. The resulting product was digested with BamHI and XhoI and ligated into pLEM019 cut with the same enzymes. This resulted in the plasmid pAKF200, which contains the *pbp2a* ORF under the control of a zinc-inducible promoter with a consensus RBS. This construct was integrated into the D39 genome at the *bgaA* site using flanking regions of homology present in the pLEM019 vector. The P_{zn}::*pbp2a* construct was fully sequenced, linearized and transformed into *S. pneumoniae* for *bgaA* integration.

P_{zn}::gfp-pbp2a. The whole pAKF200 plasmid was amplified using primers PBP2a_GFP/YFP_N_F and PBP2a_GFP/YFP_N_R. This introduced overlapping regions for isothermal assembly and a short linker sequence (coding: LEGPAGL). The *gfp* ORF was amplified using primers GFP/YFP _N_F and GFP/YFP _N_R from pUC57-*gfp*. The pUC57-*gfp* plasmid contains a *de novo* synthesized *gfp* ORF, the sequence of which was originally from a *mut2 gfp* variant in pKL134 (ref. 38) but contains additional mutations, S65A, V68L, S72A and A206K (for momomerization). It has also been codon optimized for expression of *S. pneumoniae*. These two fragments were combined by isothermal assembly, resulting in pAKF228. This plasmid was sequenced and transformed into *S. pneumoniae*. Specific integration into the *bgaA* locus was confirmed by diagnostic PCR using the BgaA_FLANK_F primer.

P_{fucose}::cozE and P_{fucose}::mreCD. The *cozE* ORF, with its native RBS, was amplified from the D39 genome using primers SPD_0768_ nativeRBS_F and SPD_0768_R. The primers introduced XhoI and BamHI sites used for insertion into pAKF205, resulting in pAKF208. To reduce *cozE* expression, pAKF208 was mutagenized to replace the ATG start codon to a sub-optimal alternative start codon (TTG) by quick-change PCR using primers SPD_0768_TTG_F/R, resulting in pAKF215. In both cases the full *cozE* ORF was sequenced. Plasmids were transformed into *S. pneumoniae* and specific integration into the *bga* locus was confirmed by diagnostic PCR using the BgaA_FLANK_F primer.

The *mreCD* ORFs, with their native RBS, were amplified from the D39 genome using primers MreC_nativeRBS_F and MreD_R. The primers introduced XhoI and BamHI sites used for insertion into pAKF205, resulting in pAKF207. The *mreCD* insert was fully sequenced and the plasmid transformed into *S. pneumoniae*. Specific integration into the *bga* locus was confirmed by diagnostic PCR using the BgaA_FLANK_F primer.

P_{fucose}::gfp-cozE and P_{fucose}::gfp-mreCD. P_{fucose}::*gfp-cozE* was cloned by isothermal assembly. The whole pAKF208 plasmid was amplified using primers SPD0768_GFP/YFP_N_5R and SPD0768_GFP/YFP_N_3F. This introduced overlapping regions for isothermal assembly and a short linker sequence (coding: LEGPAGL). The *gfp* ORF was amplified using primers GFP/YFP_N_F and GFP/YFP_N_R from pUC57-*gfp*. These two fragments were combined by isothermal assembly, resulting in pAKF218. The P_{fucose}::*gfp-cozE* construct was fully sequenced and transformed into *S. pneumoniae*. Site-specific integration into the genome at *bgaA* was confirmed by diagnostic PCR using the BgaA_FLANK_F primer. To reduce basal expression, pAKF218 was mutagenized to replace the ATG

start codon to an alternative TTG start codon by quick change PCR using primers GFP_TTG_F/R, resulting in pAKF221. The TTG mutation was sequenced and the plasmid transformed into *S. pneumoniae*.

P_{fucose}::*gfp-mreCD* was cloned by isothermal assembly. The pAKF207 plasmid was PCR amplified using primers MreC_GFP/YFP_N_5R and MreC_GFP/YFP_N_3F. This introduced overlapping regions for isothermal assembly and a short linker sequence (coding: LEGPAGL). The *gfp* ORF was amplified using primers GFP/YFP_N_F and GFP/YFP_N_R from pUC57-*gfp*. These two fragments were combined by isothermal assembly, resulting in pAKF217. The P_{fucose}::*gfp-mreC* construct was fully sequenced and transformed into *S. pneumoniae*. Site-specific integration into the genome was confirmed by diagnostic PCR using the BgaA_FLANK_F primer.

P_{zn}::*FLAG-cozE.* The triple FLAG-*cozE* fusion construct was generated by isothermal assembly. The *cozE* ORF was amplified from the D39 Δ*cps* genome using primers SPD0768_FLAG_N_F and SPD0768_FLAG_Pzn_R. These primers amplified the SPD0768 ORF (removing the start codon), added a linker (encoding: LEGPAGL) and added part of the FLAG tag. A second fragment was amplified from the D39 Δ*cps* genome using primers SPD0768_5FLANK_F and SPD0768_FLAG_N_R. These primers introduced the remaining FLAG tag sequence. The two PCR fragments were combined by isothermal assembly. The resulting reaction was further amplified using primers SPD0768_FLAG_Pzn_F and SPD0768_FLAG_Pzn_R. The assembled FLAG-SPD0768 fusion was digested with XhoI and BamHI and inserted into the pLEM023 vector cut with the same enzymes. The resulting plasmid (pAKF227) contained the codon optimized triple FLAG tag-CozE fusion under the control of the P_{zn} promoter with its native RBS.

To allow expression of two protein fusions in the same cell, we generated a strain in which the P_{zn}::FLAG-*cozE* construct was placed at the *cozE* native locus (AKF_Spn_638). A four-piece isothermal assembly was carried out consisting of a 5′-SPD0768-flanking region, P_{zn}::FLAG-SPD0768 construct, spectinomycin resistance cassette and 3′-0768-flanking region. The flanking regions were amplified from the D39 Δ*cps* genome using primers SPD0768_5FLANK_F, SPD0768_5FLANK_insert_R, SPD0768_3FLANK_F and SPD0768_3FLANK_R as appropriate. The P_{zn}-FLAG-SPD0768 construct was amplified from pAKF227 using primers pLEM023_F and pLEM023_R. Finally, the spectinomysin resistance cassette was amplified from AKF_Spn002 gDNA using primers AntibioticMarker_F and AntibioticMarker_R. The resulting assembled construct was transformed into strain AKF_Spn277 (ΔSPD0768::*erm*) and transformants selected on TSAII spec plates. Replacement of the erythromycin resistance marker with the spectinomycin marker was screened by patching candidates on TSAII erm plates. The resulting strain (AKF_Spn638) was confirmed by diagnostic PCR and sequencing using the FLAG_Seq_F primer. In addition, a diagnostic western blot was carried out to confirm FLAG-CozE expression.

Plasmid construction

pLEM019. A 5′ flanking region of the *bgaA* gene and a 3′ fragment of the *bgaA* ORF were cloned sequentially either side of a multiple cloning site (MCS). A tetracycline resistance cassette was introduced between *bgaA* regions, using a BamHI/SalI fragment of pJWV025 (ref. 37) and ligation between *bgaA* regions using the BglII/SalI sites. The resulting plasmid is an ectopic integration construct for integrating constructs at the *bgaA* locus in *S. pneumoniae*. Integration of this vector into the *S. pneumoniae* genome can be confirmed using the flanking primers BgaA_FLANK_F and BgaA_FLANK_R.

pLEM023. The zinc-inducible promoter (P_{czcD})[16] was amplified from pJWV025 (ref. 37) using primers oSp00X and oSp00Y. Primers introduced EcoRI and XhoI sites used for insertion into the pLEM019 vector cut with the same enzymes. The resulting plasmid is an ectopic integration construct for placing ORFs under the control of a zinc inducible promoter and integrating them at the *bgaA* locus in *S. pneumoniae*. Integration into the *S. pneumoniae* genome can be confirmed using the flanking primers BgaA_FLANK_F and BgaA_FLANK_R.

pAKF205. The P_{fucK} promoter characterized by Chan *et al.* was amplified from the D39 genome using primers P_fucose_F4 and P_fucose_R4 (ref. 40). The primers introduced EcoRI and XhoI sites, which were used for insertion into pLEM019 cut with the same enzymes (required partial digestion). The resulting plasmid is an ectopic integration construct for placing ORFs under the control of a fucose inducible promoter, henceforth known as 'P_{fucose}', and integrating them at the *bgaA* locus in *S. pneumoniae*.

Bacterial two-hybrid plasmids. In all cases, bacterial two-hybrid primers were given the typical name 'gene-designation'_BTH_N_F/R for N-terminal fusions and 'gene-designation'_BTH_C_F/R for C-terminal fusions. For N-terminal fusions, primers introduced XbaI sites and EcoRI for cloning into the two-hybrid vectors pKT25, pUT18 or pCH363 digested with the same enzymes[22,41]. As the ORFs of *pbp1a*, *pbp2a* and *mreC* contain EcoRI sites, primers introduced XbaI and XmaI sites for insertion into two-hybrid vectors. For C-terminal fusions, primers introduced HindIII and BamHI sites for insertion into two hybrid vectors, pKNT25 and pUT18, cut with the same enzymes[22]. All ORFs were fully sequenced before use in the two-hybrid assay.

Transposon insertion sequencing. Transposon insertion sequencing (Tn-Seq) was performed as described previously by van Opijnen and co-workers[5] with minor modifications. A total of four independently generated libraries were used in this study: two in a wt strain and two in the Δ*pbp1a* strain backgrounds. Briefly, an *in vitro* pMagellan6-Himar1 (refs 5, 42) transposon library was transformed into competent *S. pneumoniae* cells. Approximately 440,000 (wt) and 70,000 (Δ*pbp1a*) transformants were pooled for each strain and genomic DNA isolated. Samples were digested with MmeI, followed by adapter ligation. Transposon–chromosome junctions were amplified in 18 PCR cycles. PCR products were gel-purified and sequenced on the Illumina HiSeq 2500 platform using TruSeq Small RNA reagents (Tufts University Core Facility Genomics). Reads were de-multiplexed and trimmed using the CLC workbench software (Qiagen, Version 6.0.1). Sequences representing transposon-insertion sites were mapped onto the D39 genome using the short read aligner tool Bowtie[43] with a Python script (2.7.6, PSF). Bowtie aligned each sequencing run to a position on the genome, and this identified the 'TA' insertion site used by the original Mariner transposon in the libraries. The number of times each TA site was identified was scored and used to generate a read count profile across all TA sites in the genome. The read counts are sensitive to the initial number of reads from the sequencing run, so the data were normalized using a customized R-Script, normalizing the data to the library with the lowest number of reads. After normalization, a Mann–Whitney *U* test was used to identify genomic regions with significant differences in transposon insertion profiles using Python scripts (2.7.6, PSF) with both NumPy (NumPy Developers) and SciPy (SciPy developers) packages. The Mann–Whitney *U* test treats the TA insertion profile of each ORF independently, comparing them between data sets to identify genes with altered profiles. Insertion data were visualized graphically using the Artemis genome browser (version 10.2)[44]. The wt versus Δ*pbp1a* Tn-Seq data are provided in Supplementary Table 5.

Phylogenetic analysis. CozE and MreC homologues were identified using NCBI BLASTp. *S. pneumoniae* CozE and MreC protein sequences were used as queries against a database of bacterial genomes with an *e*-value cutoff of 1×10^{-4}. BLAST analysis was carried out using the Harvard Medical School research computing cluster Orchestra (https://rc.hms.harvard.edu/#orchestra).

CozE is a member of the UPF0118 family and contains no other identifiable domains. The UPF0118 family of proteins was identified by the Pfam database (version 29.0)[14]. Pfam uses multiple protein alignments to first make a *seed* alignment, and this is used to construct a profile hidden Markov model using the HMMER software. This profile is used to search sequence databases and cluster related proteins into families[15]. This approach was taken as a means of non-biased identification of CozE homologues.

In all cases, phylogenetic trees displaying the presence or absence of homologues identified by these analyses were constructed using the Interactive Tree Of Life (v3) web-based tool[45].

Fluorescent microscopy. *S. pneumoniae* cells were concentrated by centrifugation at 10,000*g* for 1 min and immobilized on 2% agarose pads. Fluorescence microscopy was performed on a Nikon Eclipse Ti-E inverted microscope through a Nikon Plan Apo ×100 oil objective (NA 1.4). For fluorescent imaging, a SPECTRA X light engine (Lumencor) was used for excitation in combination with the following filter sets for each fluorophore: GFP, Ex:475/28, Em:500–545; Dichroic: 495; TADA: Ex:438/24, Em:600–660; Dichroic: 595; TMA-DPH: Ex:390/18, Em:435-485; Dichroic: 400. Images were acquired with a CoolSnapHQ2 CCD camera (Photometrics) without gain using Nikon Elements Software (version 4.30). A neutral density 8 (ND8) filter was used to reduce the intensity of excitation light by 87.5%. Typical acquisition times were 4–7 s (GFP-PBP1a/GFP-CozE), 100–150 ms (TADA labelled cells) and 0.7–1 s (TMA-DPH stained samples).

Cell wall labelling using fluorescent D*-amino acids (TADA).* The tetramethylrhodamine(TAMRA) 3-amino-D-alanine (TADA) used in this study was synthesized by Tocris. TADA was used to label nascent *S. pneumoniae* cell wall material similar to previously described methods[20,21]. *S. pneumoniae* mid-exponential cultures (500 µl) were stained with 50 µM TADA for 15 min at 37 °C in a 5% CO_2 atmosphere. Cells were centrifuged at 10,000*g* for 1 min, washed with 500 µl phosphate-buffered saline (PBS) to remove unincorporated TADA, concentrated, immobilized on 2% PBS agarose pads and imaged immediately.

TMA-DPH membrane staining. Where TMA-DPH was used, 1 ml of culture was centrifuged at 10,000*g* for 1 min. Cells were re-suspended in 10 µl of PBS and TMA-DPH added to a final concentration of 50 µM. Cells were imaged on 2% PBS agarose pads.

Microscopy image analysis. Acquired images were processed using the Metamorph image analysis software (version 7.7.0.0). Images were cropped and scale bars added using appropriate tools. Images were corrected for background fluorescence using the subtraction feature.

Bacterial two-hybrid analysis. Competent BTH101 (Δ*cya*) *E. coli* cells were transformed with two 100 ng plasmid aliquots containing 'T25' and 'T18' protein fusions in one step. Transformants were selected on lysogeny broth (LB) agar plates containing 50 μg ml^{-1} ampicillin (Amp^{50}), 25 μg ml^{-1} kanamycin (Kan^{25}) and 40 μg ml^{-1} 5-bromo-4-chloro-3-indolyl-β-D-galactopyranoside (Xgal^{40}). Plates were incubated at 30 °C and checked for signal heterogeneity. Single colonies were picked into 150 μl LB Amp^{50} Kan^{25} containing 500 μg ml^{-1} isopropyl β-D-1-thiogalactopyranoside (IPTG^{500}) in 96 deep-well plates and incubated at 30 °C. The resulting cultures (5 μl) were spotted onto LB Amp^{50} Kan^{25} IPTG^{500} Xgal^{40} plates. Plates were incubated at 30 °C in an environment protected from light and imaged. Plates were picked in triplicate with selected images representative of three biological replicates.

Immunoblot analysis. *S. pneumoniae* cultures were normalized to an OD_{600} of 0.3 and a volume of 3 ml was harvested. Cell extracts were prepared by resuspension of cell pellets in 100 μl lysis buffer (20 mM Tris pH 7.5, 10 mM EDTA, 1 mg ml^{-1} lysozyme, 10 μg ml^{-1} DNase I, 100 μg ml^{-1} RNase A, with protease inhibitors: 1 mM phenylmethane sulfonyl fluoride [PMSF], 1 μg ml^{-1} leupeptin, 1 μg ml^{-1} pepstatin) and incubation at 37 °C for 10 min, followed by addition of 10 μl 10% sarcosyl for 5 min. SDS sample buffer (100 μl, 0.25 M Tris pH 6.8, 4% SDS, 20% glycerol, 10 mM EDTA) containing 10% 2-mercaptoethanol was added to each preparation and samples were heated for 15 min at 50 °C before loading 10 μl per lane. Proteins were separated by SDS–PAGE on 12.5% polyacrylamide gels, electroblotted onto a PVDF (polyvinylidene difluoride) membrane and blocked in 5% non-fat milk in PBS 0.5% Tween-20. The blocked membranes were probed with rabbit anti-FtsE (1:20,000)[46] and affinity-purified rabbit anti-GFP (1:10,000) diluted into 3% BSA in 1× PBS-0.05% Tween-20. Primary antibodies were detected using horseradish peroxidase-conjugated goat anti-rabbit IgG (1:20,000, BioRad) and the Western Lighning *Plus* ECL reagent as described by the manufacturer (PerkinElmer). Membrane chemiluminescence was imaged on a FluorChem R system (ProteinSimple).

Co-immunoprecipitation assay. *S. pneumoniae* strains were grown in 60 ml THY in the presence of 400 μM $ZnCl_2$ at 37 °C in 5% CO_2. These cultures (50 ml) were matched to a starting OD_{600} of 0.5. Cells were collected by centrifugation at 5,000*g* for 5 min and cell pellets were re-suspended in 25 ml SMM (1 M sucrose, 40 mM maleic acid, 40 mM $MgCl_2$, pH 6.5). Cells were washed a second time and finally re-suspended in 2 ml SMM. Cell protoplasts were generated by enzymatic digestion of the cell wall with 8 mg ml^{-1} lysozyme; cells do not lyse due to the osmotic potential of the SMM. Protoplasts were pelleted at 5,000*g* for 5 min and re-suspended in 5 ml cold hypotonic buffer 'Buffer-H' (20 mM HEPES (Na^+), 100 mM NaCl, 1 mM dithiothreitol (DTT), 1 mM $MgCl_2$, 1 mM $CaCl_2$, 1 mM phenylmethane sulfonyl fluoride (PMSF), 1 μM leupeptin, 1 μM pepstatinA). The protoplasts lysed in H-buffer due to the change in buffer osmolarity. Lysates were further treated with DNase (6 μg ml^{-1}), RNaseA (12 μg ml^{-1}) and 8 mg ml^{-1} lysozyme to form a crude extract. The extracts were pelleted by ultracentrifugation at 100,000*g* for 1 h at 4 °C. Crude membrane pellets were dispersed in 420 μl glycerol buffer 'Buffer-G' (20% glycerol, 20 mM HEPES (Na^+), 100 mM NaCl, 1 mM DTT, 1 mM $MgCl_2$, 1 mM $CaCl_2$, 1 mM PMSF, 1 μM leupeptin, 1 μM pepstatinA) and stored at −80 °C. Aliquots (50 μl) of crude membranes were solubilized with 450 μl Buffer-G-DIG (Buffer-G, 5% digitonin) for 1 h at 4 °C with gentle agitation followed by ultracentrifugation at 100,000*g* for 1 h at 4 °C. Digitonin-solubilized membrane proteins (400 μl) were incubated with anti-GFP sepharose resin for 4 h at 4 °C with slow agitation. The unbound material was removed (Flow Through) and the resin washed four times with 400 μl Buffer-G-DIG (decreasing to a final concentration of 0.05% digitonin). Proteins were eluted from the resin with 100 μl SDS–PAGE sample buffer heated to 50 °C for 15 min. Samples were denatured for 15 min at 50 °C before loading. Proteins were separated by SDS–PAGE on 15% polyacrylamide gels, electroblotted onto a PVDF membrane and blocked in 5% non-fat milk in PBS-0.5% Tween-20. The blocked membranes were probed with mouse monoclonal anti-GFP (1:5,000, Sigma) or mouse monoclonal anti-FLAG M2 (1:1,000, Sigma) diluted into 3% BSA in 1× PBS-0.05% Tween-20. Primary antibodies were detected using horseradish peroxidase-conjugated goat anti-mouse IgG (1:10,000, Biorad) and the Western Lightning Plus ECL reagent as described by the manufacturer (PerkinElmer). Membrane chemiluminescence was imaged on a FluorChem R system (ProteinSimple).

Data availability. The data that support the findings of this study are available from the corresponding authors upon request.

Received 27 March 2016; accepted 19 October 2016; published 12 December 2016

References

1. Lovering, A. L., Safadi, S. S. & Strynadka, N. C. J. Structural perspective of peptidoglycan biosynthesis and assembly. *Annu. Rev. Biochem.* **81,** 451–478 (2012).
2. Typas, A., Banzhaf, M., Gross, C. A. & Vollmer, W. From the regulation of peptidoglycan synthesis to bacterial growth and morphology. *Nat. Rev. Microbiol.* **10,** 123–136 (2011).
3. Typas, A. *et al.* Regulation of peptidoglycan synthesis by outer-membrane proteins. *Cell* **143,** 1097–1109 (2010).
4. Paradis-bleau, C. *et al.* Lipoprotein cofactors located in the outer membrane activate bacterial cell wall polymerases. *Cell* **143,** 1110–1120 (2011).
5. van Opijnen, T., Bodi, K. L. & Camilli, A. Tn-seq: high-throughput parallel sequencing for fitness and genetic interaction studies in microorganisms. *Nat. Methods* **6,** 767–772 (2009).
6. Pinho, M. G., Kjos, M. & Veening, J.-W. How to get (a)round: mechanisms controlling growth and division of coccoid bacteria. *Nat. Rev. Microbiol.* **11,** 601–614 (2013).
7. Land, A. D. & Winkler, M. E. The requirement for pneumococcal MreC and MreD is relieved by inactivation of the gene encoding PBP1a. *J. Bacteriol.* **193,** 4166–4179 (2011).
8. Hakenbeck, R. Discovery of β-lactam-resistant variants in diverse pneumococcal populations. *Genome Med.* **6,** 72 (2014).
9. Paik, J., Kern, I., Lurz, R. & Hakenbeck, R. Mutational analysis of the *Streptococcus pneumoniae* bimodular class A penicillin-binding proteins. *J. Bacteriol.* **181,** 3852–3856 (1999).
10. Gawronski, J. D., Wong, S. M. S., Giannoukos, G., Ward, D. V. & Akerley, B. J. Tracking insertion mutants within libraries by deep sequencing and a genome-wide screen for *Haemophilus* genes required in the lung. *Proc. Natl Acad. Sci. USA* **106,** 16422–16427 (2009).
11. Langridge, G. C. *et al.* Simultaneous assay of every *Salmonella Typhi* gene using one million transposon mutants. *Genome Res.* **19,** 2308–2316 (2009).
12. Job, V., Carapito, R., Vernet, T., Dessen, A. & Zapun, A. Common alterations in PBP1a from resistant *Streptococcus pneumoniae* decrease its reactivity toward β-lactams: structural insights. *J. Biol. Chem.* **283,** 4886–4894 (2008).
13. van Opijnen, T. & Camilli, A. A fine scale phenotype–genotype virulence map of a bacterial pathogen. *Genome Res.* **22,** 2541–2551 (2012).
14. Finn, R. D. *et al.* The Pfam protein families database: towards a more sustainable future. *Nucleic Acids Res.* **44,** D279–D285 (2015).
15. Tsui, H. C. T. *et al.* Suppression of a deletion mutation in the gene encoding essential PBP2b reveals a new lytic transglycosylase involved in peripheral peptidoglycan synthesis in *Streptococcus pneumoniae* D39. *Mol. Microbiol.* **100,** 1039–1065 (2016).
16. Kloosterman, T. G., van der Kooi-Pol, M. M., Bijlsma, J. J. E. & Kuipers, O. P. The novel transcriptional regulator SczA mediates protection against Zn^{2+} stress by activation of the Zn^{2+}-resistance gene *czcD* in *Streptococcus pneumoniae*. *Mol. Microbiol.* **65,** 1049–1063 (2007).
17. Lanie, J. A. *et al.* Genome sequence of Avery's virulent serotype 2 strain D39 of *Streptococcus pneumoniae* and comparison with that of unencapsulated laboratory strain R6. *J. Bacteriol.* **189,** 38–51 (2007).
18. Rice, K. C. & Bayles, K. W. Molecular control of bacterial death and lysis. *Microbiol. Mol. Biol. Rev.* **72,** 85–109 (2008).
19. Guiral, S., Mitchell, T. J., Martin, B. & Claverys, J.-P. Competence-programmed predation of noncompetent cells in the human pathogen *Streptococcus pneumoniae*: genetic requirements. *Proc. Natl Acad. Sci. USA* **102,** 8710–8715 (2005).
20. Boersma, M. J. *et al.* Minimal peptidoglycan (PG) turnover in wild-type and PG hydrolase and cell division mutants of *Streptococcus pneumoniae* D39 growing planktonically and in host-relevant biofilm. *J. Bacteriol.* **197,** 3472–3485 (2015).
21. Kuru, E. *et al. In situ* probing of newly synthesized peptidoglycan in live bacteria with fluorescent D-amino acids. *Angew. Chem. Int. Ed.* **51,** 12519–12523 (2012).
22. Karimova, G., Pidoux, J., Ullmann, A. & Ladant, D. A bacterial two-hybrid system based on a reconstituted signal transduction pathway. *Proc. Natl Acad. Sci. USA* **95,** 5752–5756 (1998).
23. Kruse, T., Bork-Jensen, J. & Gerdes, K. The morphogenetic MreBCD proteins of *Escherichia coli* form an essential membrane-bound complex. *Mol. Microbiol.* **55,** 78–89 (2005).
24. Jones, L. J. F., Carballido-López, R. & Errington, J. Control of cell shape in bacteria: helical, actin-like filaments in *Bacillus subtilis*. *Cell* **104,** 913–922 (2001).
25. Tsui, H.-C. T. *et al.* Pbp2x localizes separately from Pbp2b and other peptidoglycan synthesis proteins during later stages of cell division of *Streptococcus pneumoniae* D39. *Mol. Microbiol.* **94,** 21–40 (2014).
26. Meeske, A. J. *et al.* SEDS proteins are a widespread family of bacterial cell wall polymerases. *Nature* **537,** 634–638 (2016).
27. Cho, H. *et al.* Bacterial cell wall biogenesis is mediated by SEDS and PBP polymerase families functioning semi-autonomously. *Nat. Microbiol.* **1,** 16172 (2016).
28. Varma, A., de Pedro, M. A. & Young, K. D. FtsZ directs a second mode of peptidoglycan synthesis in *Escherichia coli*. *J. Bacteriol.* **189,** 5692–5704 (2007).
29. de Pedro, M. A., Quintela, J. C., Höltje, J. V. & Schwarz, H. Murein segregation in *Escherichia coli*. *J. Bacteriol.* **179,** 2823–2834 (1997).
30. Aaron, M. *et al.* The tubulin homologue FtsZ contributes to cell elongation by guiding cell wall precursor synthesis in *Caulobacter crescentus*. *Mol. Microbiol.* **64,** 938–952 (2007).

31. Hoskins, J. *et al.* Genome of the bacterium *Streptococcus pneumoniae* strain R6. *J. Bacteriol.* **183,** 5709–5717 (2001).
32. Avery, O. T., MacLeod, C. M. & McCarty, M. Studies on the chemical nature of the substance inducing of transformation of pneumococcal types: induction of transformation by a desoxyribonucleic acid fraction isolated from *Pneumococcus* type III. *J. Exp. Med.* **79,** 137–158 (1944).
33. Robertson, G. T., Ng, W. L., Foley, J., Gilmour, R. & Winkler, M. E. Global transcriptional analysis of clpP mutations of type 2 *Streptococcus pneumoniae* and their effects on physiology and virulence. *J. Bacteriol.* **184,** 3508–3520 (2002).
34. Gibson, D. G. *et al.* Enzymatic assembly of DNA molecules up to several hundred kilobases. *Nat. Methods* **6,** 343–345 (2009).
35. Hava, D. L., Hemsley, C. J. & Camilli, A. Transcriptional regulation in the *Streptococcus pneumoniae rlrA* pathogenicity islet by RlrA. *J. Bacteriol.* **185,** 413–421 (2003).
36. Sung, C. K., Li, H., Claverys, J. P. & Morrison, D. A. An *rpsL* cassette, janus, for gene replacement through negative selection in *Streptococcus pneumoniae*. *Appl. Environ. Microbiol.* **67,** 5190–5196 (2001).
37. Eberhardt, A., Wu, L. J., Errington, J., Vollmer, W. & Veening, J. W. Cellular localization of choline-utilization proteins in *Streptococcus pneumoniae* using novel fluorescent reporter systems. *Mol. Microbiol.* **74,** 395–408 (2009).
38. Lemon, K. P. & Grossman, A. D. Localization of bacterial DNA polymerase: evidence for a factory model of replication. *Science* **282,** 1516–1519 (1998).
39. Sung, M.-T. *et al.* Crystal structure of the membrane-bound bifunctional transglycosylase PBP1b from *Escherichia coli*. *Proc. Natl Acad. Sci. USA* **106,** 8824–8829 (2009).
40. Chan, P. F. *et al.* Characterization of a novel fucose-regulated promoter (PfcsK) suitable for gene essentiality and antibacterial mode-of-action studies in *Streptococcus pneumoniae*. *J. Bacteriol.* **185,** 2051–2058 (2003).
41. Bendezú, F. O., Hale, C. A., Bernhardt, T. G. & de Boer, P. A. J. Rodz (YfgA) is required for proper assembly of the MreB actin cytoskeleton and cell shape in *E. coli*. *EMBO J.* **28,** 193–204 (2009).
42. Lampe, D. J., Akerley, B. J., Rubin, E. J., Mekalanos, J. J. & Robertson, H. M. Hyperactive transposase mutants of the Himar1 mariner transposon. *Proc. Natl Acad. Sci. USA* **96,** 11428–11433 (1999).
43. Langmead, B., Trapnell, C., Pop, M. & Salzberg, S. L. Ultrafast and memory-efficient alignment of short DNA sequences to the human genome. *Genome Biol.* **10,** R25 (2009).
44. Carver, T., Harris, S. R., Berriman, M., Parkhill, J. & McQuillan, J. A. Artemis: an integrated platform for visualization and analysis of high-throughput sequence-based experimental data. *Bioinformatics* **28,** 464–469 (2012).
45. Letunic, I. & Bork, P. Interactive Tree of Life (iTOL): an online tool for phylogenetic tree display and annotation. *Bioinformatics* **23,** 127–128 (2007).
46. Meisner, J. *et al.* FtsEX is required for CwlO peptidoglycan hydrolase activity during cell wall elongation in *Bacillus subtilis*. *Mol. Microbiol.* **89,** 1069–1083 (2013).

Acknowledgements

The authors thank all members of the Bernhardt and Rudner laboratories for support and comments. A. Fenton was a jointly mentored postdoctoral fellow bridging work in both laboratories. The authors thank R. Yunck, H. Kimsey, M. Winkler, T. van Opijnen, A. Camilli, N. Campo, J.-W. Veening, T. Vernet and D. Morrison for strains, reagents and technical assistance. This work was supported by the National Institutes of Health (R01AI083365 to T.G.B., CETR U19 AI109764 to T.G.B. and D.Z.R., GM073831 to D.Z.R. and RC2 GM092616 to D.Z.R.).

Author contributions

A.K.F. performed all experiments, designed part of the experimental programme and co-authored the manuscript. L.E.M. carried out essential pilot experiments for the project. D.T.C.L. helped adopt the Tn-seq data analysis pipeline and proofread the manuscript. D.Z.R. and T.G.B. co-supervised the project and co-authored the manuscript.

Additional information

Supplementary information is available for this paper.

Reprints and permissions information is available at www.nature.com/reprints.

Correspondence and requests for materials should be addressed to D.Z.R. and T.G.B.

How to cite this article: Fenton, A. K., El Mortaji, L., Lau, D. T. C., Rudner, D. Z. & Bernhardt, T. G. CozE is a member of the MreCD complex that directs cell elongation in *Streptococcus pneumoniae*. *Nat. Microbiol.* **2**, 16237 (2016).

Competing interests

The authors declare no competing financial interests.